Working memory load related theta power decreases in dorsolateral prefrontal cortex predict individual differences in performance

A Brzezicka[1,3], **J Kami ski**[1,4], **CM Reed**[2], **JM Chung**[2], **AN Mamelak**[1], **U Rutishauser**[1,2,4]

[1]Department of Neurosurgery, Cedars-Sinai Medical Center, Los Angeles, California, USA.
[2]Department of Neurology, Cedars-Sinai Medical Center, Los Angeles, California, USA.
[3]Department of Psychology, SWPS University of Social Sciences and Humanities, Warsaw, Poland. [4]Division of Biology and Biological Engineering, California Institute of Technology, Pasadena, California, USA

Abstract

Holding information in working memory (WM) is an active and effortful process that is accompanied by sustained load-dependent changes in oscillatory brain activity. These proportional power increases are often reported in EEG studies recording theta over frontal midline sites. Intracranial recordings, however, yield mixed results depending on the brain area being recorded from. We recorded intracranial EEG with depth electrodes in 13 patients with epilepsy that were performing a Sternberg WM task. Here, we investigated patterns of theta power changes as a function of memory load during maintenance in three areas critical for WM: dorsolateral prefrontal cortex (DLPFC), dorsal anterior cingulate cortex (dACC) and hippocampus. Theta-frequency power in both hippocampus and dACC increased during maintenance. In contrast, theta-frequency power in the DLPFC decreased during maintenance and this decrease was proportional to memory load. Only the power decreases in DLPFC, but not the power increases in hippocampus and dACC, were predictive of behavior in a given trial. The extent of the load-related theta power decreases in the DLPFC in a given subject predicted a subject's reaction times, revealing that DLPFC theta explains individual differences in WM ability between subjects. Together, this data reveals a pattern of theta power decreases in the DLPFC that is predictive of behavior and that is opposite of that in other brain areas. This result suggests that theta band power changes serve different cognitive functions in different brain areas and specifically that theta power decreases in DLPFC have an important role in maintenance of information.

Keywords

theta power; power decrease; dorsolateral prefrontal cortex; hippocampus; Sternberg task; working memory; iEEG; individual differences

Corresponding author: ueli.rutishauser@cshs.org.

INTRODUCTION

Maintaining information in the absence of external stimuli is crucial for many cognitive functions (Unsworth & Engle, 2006, 2007). The ability to actively hold a piece of information in mind and resist interference forms the core of the working memory system (WM) (Baddeley, 2010). The capacity of an individual's WM is predictive of that persons cognitive ability in a number of domains, including analytic problem solving (Wiley, & Jarosz, 2012), reading (Nouwens, Groen, & Verhoeven, 2017), and fluid intelligence (Shipstead, Harrison, & Engle, 2016), a finding that highlights the broad importance of WM for someone's overall cognitive abilities.

Holding information in WM is an active and effortful task that is thought to depend on the large-scale interaction of multiple brain areas. This interaction is thought to be coordinated by synchronized oscillations, a view supported by the finding that the maintenance of information in WM leads to substantial changes in the oscillatory activity of field potentials in many brain areas. Theta-frequency (3–8Hz) band power increases are among the most consistently documented during WM maintenance. This increase was found in many areas, including medial prefrontal cortex (PFC), the hippocampus (Axmacher et al., 2010; Maurer et al., 2015; Onton, Delorme, & Makeig, 2005; Tesche & Karhu, 2000; Tsujimoto, Shimazu, Isomura, & Sasaki, 2010), and sensory areas (Lee, Simpson, Logothetis, & Rainer, 2005). The magnitude of this increase in theta power is typically proportional to the amount of the information being held in mind, with higher loads and/or higher effort resulting in higher theta-band power (Gärtner, Grimm, & Bajbouj, 2015; Howard, 2003; Jensen & Tesche, 2002; Maurer et al., 2015; Meltzer et al., 2008; Wisniewski et al., 2015). Also, theta-band power changes are predictive of behaviors that depend on WM (Lega, Jacobs, & Kahana, 2012; Womelsdorf, Johnston, Vinck, & Everling, 2010; Zakrzewska & Brzezicka, 2014), a result that shows that theta band activity is functionally relevant for this kind of cognitive activity.

An extensive body of literature indicates that medial frontal cortex, dorsal lateral prefrontal cortex (DLPFC), and the hippocampus serve important roles in WM maintenance. However, the distinct roles of each in WM is poorly understood. While extensively observed in scalp EEG studies (Meltzer, Negishi, Mayes, & Constable, 2007; Roux & Uhlhaas, 2014), and specifically for frontal midline theta (FMT) (Asada, Fukuda, Tsunoda, Yamaguchi, & Tonoike, 1999; Gärtner et al., 2015; Maurer et al., 2015; Mitchell, McNaughton, Flanagan, & Kirk, 2008; Onton et al., 2005), it remains unclear which brain areas specifically contribute to the observed theta-power increases in scalp EEG. Because each EEG electrode is sensitive to electrical fields generated by large populations of neurons that may be spatially distributed, there is not necessarily a one-to-one mapping between scalp electrode location and the source of the underlying neural activity. Consequently, the scalp FMT power changes are likely a mixture of activity in many areas, including the hippocampus.

To better differentiate the distinct contributions of different areas to WM, direct intracranial recordings are crucial. Here, we simultaneously recorded from all three, key for WM, areas using intracranial recordings in epilepsy patients implanted with depth electrodes. We then characterize and compare the properties of theta during WM maintenance in each region.

The principle goal of this study is two-fold: First, to determine whether medial frontal (dorsal part of the anterior cingulate cortex, dACC), lateral prefrontal (DLPFC), and medial temporal (hippocampus) areas show similar or differential patterns of changes in theta power during WM maintenance. Second, to quantify which of these theta-changes predicts behavior.

Of particular interest in this study is the DLPFC, which is thought to be a key structure in coordinating – via oscillatory dynamics – large-scale neuronal interactions in a task-depended manner (Helfrich & Knight, 2016). Oscillatory mechanisms underlying simple cognitive processes were first described in the hippocampus and primary sensory areas of rodents and nonhuman primates, but recent works suggest that higher cognitive processes, including WM, are also facilitated by similar oscillatory mechanisms (Helfrich & Knight, 2016; Wang, 2010). Single-neuron, intracranial, fMRI, and lesion evidence indicates that the dorsolateral prefrontal cortex (DLPFC) plays an essential role in WM maintenance (Altamura et al., 2007; Curtis & D'Esposito, 2003; Manoach et al., 1997; Michels et al., 2010b; Rottschy et al., 2012). For example, the BOLD-fMRI signal in DLPFC is parametrically related to both increases in memory load and task complexity (Altamura et al., 2007; Jansma, Ramsey, De Zwart, Van Gelderen, & Duyn, 2007; Manoach et al., 1997; Michels et al., 2010a; Rottschy et al., 2012). Similarly, single neurons in DLPFC in macaques exhibit stimulus-selective persistent neural firing across the delay period of WM task (Funahashi, 2017; Fuster, 1973; Fuster & Alexander, 1971; Goldman-Rakic, 1995; Lara & Wallis, 2015; Riley & Constantinidis, 2016). Signatures of such "persistent" activity in DLPFC have also been observed using fMRI in humans (Curtis & D'Esposito, 2003). The importance of human DLPFC in WM is further supported by the effects of stimulating DLPFC with TMS, which can result in profound changes in WM task performance. Depending on the stimulation protocol, such stimulation can result in either enhanced (Bagherzadeh, Khorrami, Zarrindast, Shariat, & Pantazis, 2016) or decreased WM performance (Morgan, Jackson, Van Koningsbruggen, Shapiro, & Linden, 2013; Schicktanz et al., 2015). The specific role of the DLPFC in WM is thought to be of an executive – compared to a simple maintenance – nature, i.e. it is thought to coordinate and control other WM-related areas, including the hippocampus.

Hippocampal involvement in WM depends on task duration and complexity (Yoon, Okada, Jung, & Kim, 2008) and changes as a function of age (Finn, Sheridan, Kam, Hinshaw, & D'Esposito, 2010). In contrast, PFC appears to be essential for WM task performance at any age and for a wider range of tasks. Moreover, it seems that the DLPFC is primarily engaged in maintaining and processing of information lasting from milliseconds to several seconds, whereas the hippocampus is crucial when working memory demands are more complex and/or when maintenance duration is longer (Yoon et al., 2008). In addition, animal studies show that both hippocampal and prefrontal activity during WM tasks is critical (Bähner et al., 2015; Spellman et al., 2015; Yoon et al., 2008). In humans, persistently active cells during WM maintenance have been observed in both the hippocampus and the medial frontal cortex (MFC), but the properties of these cells differ between the two areas. While persistent activity was observed in both areas, such activity was only stimulus selective in the hippocampus (Kami ski et al., 2017). In contrast, persistent activity in MFC was sensitive to load and memory-quality, but not stimulus identity. Together, this existing

literature indicates that studying the distinct contributions of different brain areas to WM maintenance is a powerful way to differentiate what a particular area contributes to WM.

While there is extensive evidence for a role of the DLPFC in WM, it remains unknown whether theta-band power in DLPFC is modulated by WM and whether such theta-band changes are similar to those observed in the MFC and hippocampus. Here, we utilize intracranial recordings to directly compare the degree of modulation of theta-band power in these three areas. We identified contacts placed in the DLPFC in 13 neurosurgical patients and compared the intracranial EEG (iEEG) recorded from these to those obtained from contacts placed in the hippocampus and dACC in the same patients. We found that DLPFC theta-band exhibited prominent load-related power decreases, a pattern of change markedly different from that found in hippocampus and dACC. These power-decreases were predictive of behavior in a given trial as well as individual differences between subjects, indicating that these power reductions were significant for WM maintenance. Together, our results raise the intriguing question of how reductions in power in a given frequency band can be beneficial for the contribution of an area to a particular cognitive function.

METHODS

Participants

We recorded intracranial EEG from thirteen patients (14 sessions) implanted with depth electrodes for possible surgical treatment of epilepsy. We previously reported single-neuron recordings in the MTL and MFC from a subset of the same patients in the same task (Kami ski et al., 2017). Here, in contrast, our focus is on the iEEG signal, in particular on the DLPFC. The average age of our subjects was 37.46 (SD = 16.2, 17 to 70 y), seven patients were male (see Table 1). Patients volunteered for the study and provided informed consent. This study was approved by the Institutional Review Board of the Cedars-Sinai Medical Center.

Localization of electrodes—All electrodes were localized based on pre- and postoperative T1 structural MRIs. We used the following processing pipeline to transform the postoperative MRI into the same space as a template brain. We extracted the brains from the pre- and postoperative T1 (Ségonne et al., 2004) scans and aligned the postoperative scan to the preoperative scan with Freesurfer (https://surfer.nmr.mgh.harvard.edu/) "MRI_Robust_Register" algorithm (Reuter, Rosas, & Fischl, 2010). We then computed a forward mapping of the preoperative scan to the CIT168 template brain (Tyszka & Pauli, 2016) using a concatenation of an affine transformation followed by a symmetric image normalization (SyN) diffeomorphic transform, computed by the ANTs software package (Avants et al., 2008). This resulted in a postoperative scan overlaid on a version of the CIT168 template brain (Tyszka & Pauli, 2016) registered in MNI152 space.

We have described our electrode localization procedures for amygdala, hippocampus, and dACC previously (Kami ski et al., 2017; Minxha et al., 2017; Minxha, Mamelak, & Rutishauser, 2018). We have not previously documented our procedures for DLPFC, which are as following. We compared the locations of putative DLPFC contacts to landmarks that

define the boundaries of DLPFC (in Freesurfer Freeview). The boundaries we used followed the standard recommendations for TMS navigation (Mylius et al., 2013): we included electrodes placed in the middle frontal gyrus (MFG) between the superior frontal sulcus (SFS) and inferior frontal sulcus (IFS) (the middle of the line separating the anterior and middle thirds of the MFG, see (Mylius et al., 2013)). Such location is also in accordance to other definitions based on cytoarchitectonic approach, where DLPFC is defined as Brodmann areas 46 and 9 (Rajkowska & Goldman-Rakic, 1995). Note, that here we included only contacts in MFG for analysis. However, DLPFC proper also extends into SFG (BA9), but no such contacts were included here. It is thus important to note that the results here only pertain the part of DLPFC located in MFG. The location of each contact was confirmed visually and only contacts located within the defined boundaries were included in the analyses. Applying this approach resulted in 46 contacts identified as DLPFC contacts (2–4 per subject, across both hemispheres; 0–2 per hemisphere). For dACC and hippocampus, we took the most medial contacts (clinical contact closest to the microwires) on the electrodes targeting the dACC and hippocampus (for each, we confirmed proper microwire placement in the targeted area), respectively. In total, we identified 26 dACC and 23 hippocampus contacts.

For visualization purposes only, electrode locations were projected into MNI152 space and projected onto a 2D plane by collapsing across the third axis (Fig 1D–E.). MNI coordinates for all electrodes are given in Table 2.

Stimuli and Procedures

Task—Subjects performed a working memory task ("Sternberg" task, based on (Sternberg, 1966)). In each trial subjects were asked to remember between one up to three sequentially presented pictures. Then, after 2.5–2.8s of maintenance period they were presented with another picture and asked if they have seen it or not. We used a modified Sternberg task with images (instead of the usual digits) as material for memorization (Fig. 1a). Each trial started with a fixation cross shown for 900–1,000 ms. Next, we sequentially presented the images to be memorized ('encoding') in a given trial. Each picture was presented for 1 s, followed by a blank screen for 1–200 ms (randomized). Subjects were asked to memorize the 1–3 images shown in each trial. After encoding, there was a maintenance (delay) period lasting at least 2.5 s and at most 2.8 s. During this time, the word "hold" was shown on the screen. Lastly, after the end of the maintenance period, a probe stimulus was displayed, and subjects were asked to decide whether the probe stimulus has been presented in the encoding phase. Participants responded by pressing the green or red buttons on a response pad. Which color corresponded to 'yes' and which to 'no' was shown at the top of the screen during each probe trial (Fig. 2). We used this approach to switch the location of the yes and no buttons in the middle of the experiment as a control. We asked subjects to respond as fast as possible. The probe picture was presented until subjects made a response. In each session, subjects performed 108 (first subject) or 135 (all subjects except the first one) trials depending on the task variant (we changed the number of trials from 108 to 135 after the first subject). Pictures were shown in pseudorandom order. A schematic overview of the task is shown in the Figure 2. The number of pictures presented in a given trial was unknown to the participant (the load variable was mixed within blocks).

iEEG Measurement and Analysis—We recorded broadband (0.1–500 Hz filter) and continuous signals from all channels sampled at 2 kHz using a Neuralynx Atlas system. Recordings were referenced to a subgaleal reference electrode strip (Minxha et al., 2018). Data analysis was performed off-line using EEGLAB toolbox (Delorme & Makeig, 2004) and custom MATLAB (The MathWorks, 2015) scripts. The continuous iEEG was downsampled to 500 Hz and the recording channels of interest were re-referenced to bipolar by subtracting the signal of the contact closest to the channel of interest (see Fig 1). For DLPFC electrodes, this was the immediate next medial channel to the channel of interest (see Fig. 1B and 1C), whereas for hippocampus and dACC this was the immediate next lateral channel on the same electrode. Next, we Z-transformed the signal of each channel separately. The 4500 ms long epochs were then extracted from the maintenance period of every trial (starting 1000 ms before the start of maintenance till 1000 ms after the end of the maintenance period, which lasted at least 2500ms) and 3000 ms epochs were extracted from the picture presentation period (encoding) as well as from the retrieval period (starting 1000 ms before and ending 1000 ms after the actual 1000 ms lasting periods of interest). For the baseline, we extracted a 2000ms long segment for every trial (1000 ms before up to 500 ms after the actual baseline period which was defined as a 500 ms period time with fixation cross before the first picture presentation – see Fig. 2 where it is marked as a blue shading on the experiment's time line). All trials were visually inspected for artifacts and rejected if found to contain artifacts (with an average of 87 % (+/− 0.8%) of epochs remaining in the analysis). We used the Morlet continuous wavelet transform (CWT; 16 scales per octave, minimum period to analyze was set to 0.01 and maximum period was set to 0.8) as implemented in WAVOS (Wavos 2.3.1) to calculate the absolute power spectral density for every trial. We first computed the CWT on the entire trial and then extracted the periods of interest as described above. Finally, we transformed the units of power to decibels relative to the average power during the baseline period.

Statistical Analyses—For comparisons between two conditions, we used the permuted t-test statistic. For comparisons with more than two conditions, we used permuted F-statistic. Note that we used permutation tests throughout to avoid the assumption of normality. As a result, note that the reported P-values may differ from those expected from the parametric t- and F-distributions because P-values were based on the empirically estimated null distribution. We used corrections for multiple comparisons based on cluster-based approach (Maris & Oostenveld, 2007), when appropriate. For linear mixed effects models and correlation analysis, we used Matlab's FITLME function, and Spearman rho, respectively.

Results

Behavioral data—Subjects (N=13 in 14 sessions) performed the task well: overall accuracy was 87.57 % ± 4.33%, with a median reaction time (for correct trials only) of 1.07 ± 0.27sec. As expected (Sternberg, 1966), accuracy decreased (Fig. 3A, $F_{(2,26)}=3.65$; p=0.037, permuted repeated-measures ANOVA) and reaction time (RT) increased (Fig. 1B, $F_{(2,26)}=6.69$; p=0.0025, permuted repeated-measures ANOVA) as a function of the number of items held in memory (here referred to as load). Also, RT was significantly faster for correct compared to incorrect trials (Fig. 3C; permuted paired t-test: $t_{(13)}=6.26$; p=0.005, using trials from load 3 only due to low error rates for low loads; average error rates were

0.066, 0.093, and 0.12 for load 1–3, respectively). Together, this pattern of behavioral results shows that our patients performed the task accurately and exhibited the expected patterns of accuracy and reaction time differences (Sternberg, 1966). For all subsequent analysis, we used only correct trials unless indicated otherwise. We did observe minor but non-significant priority and recency effects (in load 3 trials the image presented last was recognized faster (M= 1.16 s) than the image presented in the middle (M= 1.32 s)). Similarly, the image presented first during encoding was recognized faster (M= 1.23 s) relative to the middle image. However, these differences were not statistically significant (F(2,26)=1.47; p=0.25).

Electrophysiology—Across 13 patients, we recorded from in total 46, 26, and 23 channels in DLPFC, dACC, and hippocampus, respectively (see methods and Table 1). We localized electrode contacts based on post-operative MRI scans and only included channels confirmed to be in either area (see methods and Fig. 1 for definition of what we included as DLPFC). All analyses conducted in this paper was performed on bipolar-referenced recordings (referenced to the immediate next contact relative to the one of interest, see methods).

Changes in power spectrum during maintenance versus baseline—As a first step, we compared whether the patterns of power changes during the maintenance period relative to the baseline period differed between brain areas. We performed a permuted 1×3 ANOVA for power at each frequency, corrected for multiple comparisons using a cluster based approach (Maris & Oostenveld, 2007). Results at p < 0.05 were considered statistically significant. Averaging across all loads, we found that the pattern of response in the broadband power varied systematically between the three brain areas investigated here. Whereas in DLPFC we found broadband decreases relative to baseline, in both dACC and hippocampus we observed significant power increases relative to baseline (Fig. 4A). In a pairwise comparison between the brain areas, this difference was significant between DLPFC and hippocampus in the 1–20 Hz band(Fig. 4B). Comparing between DLPFC and dACC, power was significantly different in the 1–15 Hz band(Fig. 4C). In contrast, differences between dACC and hippocampus were only significant in the 12–20Hz band, with no significant differences in the 1–5Hz band (Fig. 4D). Together, this shows significant and relatively broad-band power deceases in DLFPC and power increases in the dACC and hippocampus during WM maintenance relative to baseline. As a further control, we also assessed whether the raw power (rather than subtracted from baseline or between loads, as reported above) in DLPFC differed relative to that expected from the background 1/f spectrum. This revealed that (Fig. 4E) raw power differed significantly from the background in both the theta and beta frequency band and that the power-decreases relative to baseline were also apparent in the raw spectra.

Changes in theta power as a function of load—We next investigated whether maintenance-related activity varied as a function of load, a strategy commonly used in investigating the mechanisms of WM (Hsieh & Ranganath, 2014; Meltzer et al., 2008; Onton et al., 2005; Roux & Uhlhaas, 2014). So, in the next analysis we asked whether the power increases/decreases we described above scaled as a function of load by comparing the magnitude of change between high (3 items) and low (1 item) load conditions (Fig. 5). This

revealed that the extent of DLPFC power decreases was a function of load, with the largest decrease for the high load condition (permuted ANOVA, p= 7.1418e-05, 3.29–6.86 Hz, corrected for multiple comparisons). In contrast, the higher the load, the larger the increase in theta-band power in the hippocampus (permuted ANOVA, p=0.038, 2.43–3.91 Hz, without correction for multiple comparisons, after correction all effects were statistically non-significant). It was notable that the effect size was substantially larger in the DLPFC relative to the hippocampus (d_{DLPFC}=0.961, $d_{HIPPOCAMPUS}$=0.477). An additional difference was that the load modulation in DLPFC was most apparent in a higher frequency compared to the hippocampus (5 Hz vs. 3.5 Hz). Lastly, the pattern of response in the dACC did not vary significantly as a function of memory load (but note that relative to baseline power increased significantly in the dACC, but this change was not a function of load). Together, this shows that the power increases and decreases in hippocampus and DLPFC during maintenance were modulated significantly by memory load, but this modulation was of opposite sign for DLPFC (negative) compared to hippocampus (positive). This analysis also shows that, in contrast to the comparison maintenance period vs. baseline, the load-related scaling was specific to the theta-frequency band (the first, more general comparison revealed a broadband effects).

We next asked whether the extent of theta power increase/decrease was indicative of memory load for individual electrodes (rather than averaged across as shown above). For this analysis, we averaged power in the frequency of interest (3–6 Hz theta band) for each electrode and for each memory load separately. We then performed a 3 (Memory load: 1 picture vs 2 pictures vs 3 pictures) x 3 (Area of interest: DLPFC vs dACC vs Hippocampus) repeated measures ANOVA with theta power as the dependent variable. We found that the main effects of Memory load [$F(2,200) = 4.46$, $p = .013$, eta2 = .043] and Brain area [$F(2,100) = 15.086$, $p < .0001$, eta2 = .232] as well as the interaction [$F(4,200) = 10.73$, $p < .0001$, eta2 = .177] were statistically significant, demonstrating the robustness of this effect at the single-electrode level. The significant interaction effect was due to the opposite pattern of effects for DLPFC [see Fig. 6A; where we observed a significant, negative linear trend: $F(1,49) = 49.24$, $p < .0001$, eta2 = .501] compared to hippocampus [see Fig. 6B; where the trend was significant but much weaker and positive $F(1,24) = 5.18$, $p = .032$, eta2 = .178] and dACC [see Fig. 6C; F < 1, ns.]. See also Fig. 8 for additional single-channel presentation of this effect.

We next confirmed this conclusion at the single-trial level. For this, we used a linear mixed effects model with memory load and brain area as fixed factors and channels as random factors. Theta power in each trial constituted the dependent variable. The goal of this analysis was to confirm the brain area x memory load interaction on the single trial level. We found that the interaction term was highly significant ($F(1,11950) = 45.55$, $p = 1.5584e-11$). This confirms the robustness of the opposite effects of load on theta power in the DLPFC versus dACC/Hippocampus at the single-trial level.

We performed several control analysis to exclude potential confounds. First, we verified whether evoked responses (ERPs) to the onset of the waiting period ("hold" instruction) differed between loads. To do so, we averaged the raw signal across trials from each load separately and then submitted these ERPs to a permuted repeated measures ANOVA (we

compared ERPs independently at every point of time, corrected for multiple comparisons using a cluster based approach (Maris & Oostenveld, 2007)). This analysis revealed that ERPs from different loads did not differ statistically significant at any point of time. Second, we confirmed that those evoked responses did not cause the reported load-related theta power changes in DLPFC. To achieve this, we subtracted the ERPs from each individual trial of a given load and repeated the above analysis on the resulting ERP-subtracted trials. Compatible with the original analysis, this again revealed a significant effect of memory load on DLPFC theta power: $F(2,98) = 31,28$; $p < .0001$ [$M_{load1} = -.54$; $M_{load2} = -.68$; $M_{load3} = -.84$]. In comparison, the effect sizes of the original analysis (where the ERP was not subtracted) were similar ($F(2,98) = 30,41$; $p < .0001$ [$M_{load1} = -.93$; $M_{load2} = -1.06$; $M_{load3} = -1.23$]). Together, this shows that the load-dependent theta power decrease in the DLPFC was not related to an evoked response.

Time course of DLPFC power changes—We next investigated how theta power in the DLPFC is changing over the course of the task. We were especially interested in whether changes in theta power were also visible during the encoding or retrieval stage and how power changes evolved throughout the maintenance period. We found that throughout the maintenance period, theta band power scaled as a function of load, with less power for higher loads (Fig. 7A, middle). Also, during encoding, theta-band power dropped in a step-wise fashion as more items were encoded (Fig. 7A, left). Notable, neither the beta (see Fig. 7B) nor the gamma (see Fig. 7C) frequency-band showed similar load-related changes during maintenance.

Theta power as a predictor of task performance—In the analysis above, we considered only correct trials. We next asked whether there is a relationship between theta power and performance (we tested accuracy and RT). To test for effects of accuracy, we used a linear mixed effects model. We used brain area and accuracy (correct/incorrect) as fixed factors, channel number as a random factor, and single-trial theta power as the dependent variable. We only used load 3 trials for this analysis (to have enough error trials). This model revealed significant main effects of both brain area $F(1,4106) = 9.56$, $p = 0.0019$ (as expected from above analysis) and accuracy $F(1,4106) = 7.61$, $p = 0.0058$, and a significant interaction between the two ($F(1,4106) = 3.87$, $p = 0.049$). Post-hoc analysis revealed a significant difference between correct and incorrect trials only in DLPFC, in which correct trials were characterized by lower theta power compared to incorrect trials ($F(1,1982) = 12.87$, $p = 0.00034$). We found no significant difference between correct and incorrect trials for theta power in hippocampus and dACC ($F(1,1004) < 1$, ns. and $F(1,1118) < 1$, ns., respectively, see Fig. 9A–C). Together, this shows that the extent of theta power decreases in DLPFC is predictive of accuracy, with less power indicative of a higher likelihood of a correct response.

To test for effects of RT, we performed a similar analysis but using only correct trials from all loads. We first ran a linear mixed effects model with raw reaction times (removing outliers, see methods) and brain area as fixed factors, channels as random factor and theta power as the dependent variable. This analysis revealed significant main effects of brain area ($F(1, 9980) = 70.51$; $p = 5.2158e\text{-}17$), reaction times ($F(1, 9980) = 5.96$; $p = 0.015$), as well

as a significant interaction (F(1, 9980) = 13.86; p = 0.00019). Post-hoc analysis revealed that the interaction effect was due to the opposite sign of the relationship between theta power and reaction times in DLPFC (Fig. 9D; r = 0.052, p = 3.2949e-04) as compared to hippocampus (Fig. 9E; r = −0.056, p = 0.0053) and dACC (Fig. 9F; r = −0.04, p = 0.0358).

To exclude potential confounds of load on RT (the larger the load, the longer the RT), we repeated above analysis after first classifying RTs as below/above the median RT for each load of a given patient. Thus, for each load, a trial was labeled as either "faster" or "slower" relative to the median RT of that load (a technique we used before (Kami ski et al., 2017)). This analysis yielded very similar results: there were significant main effects of brain area (F(1, 9980) = 67.19; p = 2.7753e-16), RT (F(1, 9980) = 12.17; p = 0.00049), and a significant interaction (F(1, 9980) = 14.39; p = 0.00015) resolving the question about the memory load as a potential confound variable. Post-hoc analysis again confirmed the opposite signs of modulation due to RT of DLPFC relative to hippocampus and dACC (positive in DLPFC, r = 0.052, p = 3.2949e-04; negative in Hippocampus, r = −0.056, p = 0.0053; negative in dACC, r = −0.04, p = 0.0358). Together, this analysis shows a robust relationship between decreases in theta power in the DLPFC with both accuracy and RT. The directionality of this effect in the DLPFC was such that the more theta power was reduced, the faster and more accurate was the response. In contrast, faster RTs in the hippocampus and dACC were correlated with increases in theta power and such increases did not correlate significantly with increases in accuracy.

Individual differences in load-related theta power changes as a predictor of task performance—We next tested whether the amount of load-related changes in theta power is related to individual differences in RT and accuracy between subjects. Note that in contrast to the within-subject analysis presented so far, what follows is a between subject analysis. As the neural metric of interest, we again used the difference between theta power in load 3 relative to load 1 (for each channel). To quantify behavior, we used accuracy and reaction time for each subject. We used a linear mixed effects models with the change in theta power and brain area as predictors and reaction times or accuracy as the dependent variable.

For RT, we found a significant main effect of theta power change (F(1,99)=6.22, p = 0.014) and brain area (F(1,99) = 4.84, p = 0.036), with no significant interaction between the two (F(1,99) = 2.53, p = 0.115). When we repeat this analysis with RT from the load 3 only (the most difficult condition) the both main effects were of similar magnitude, F(1,99)=6.98, p = 0.009 for theta change and brain area F(1,99)=4.8, p = 0.031 but interaction effect became marginally significant, F(1,99)=3.56, p = 0.062. To explore this relationship in more depth, we conducted post hoc analyses with only one predictor (theta change) for each area separately. This analysis revealed that the extent of theta power change was predictive of RTs, but only for DLPFC (F(1,48) = 13,19, p = 0.00068 for RTs from all correct trials and F(1,48) = 12,82, p = 0.00079 for RT from load 3). In contrast, for hippocampus and dACC this effect was not significant (see Fig. 10B–C, F(1,23) <1, ns. For hippocampus and F(1,26)<1, ns. for dACC). We next repeated this analysis with accuracy as the dependent variable. This revealed no significant correlation between accuracy and theta power changes in any of the three brain areas.

Together, these results show a significant positive correlation between the amount by which DLPFC theta power decreased as a function of memory load and the mean reaction time of a subject. Thus, the bigger the decrease with memory load was for a given subject during the maintenance period, the faster the response was of that subject (see Fig 10; this was true for RTs in all loads). These results thus reveal that the extent of DLPFC theta power decreases explain individual differences in RT in a working memory task.

Discussion

The main aim of this study was to compare theta power changes as a function of memory load during WM maintenance between three brain areas: the DLPFC, the hippocampus and the dACC. The reason for doing so is that these three areas have long been thought to be critical for WM (Bähner et al., 2015; Barbey, Koenigs, & Grafman, 2013; Lenartowicz & McIntosh, 2005), but it remains unclear how each of these areas contributes to information maintenance in WM. While our study cannot claim to answer this question, the differences we identify here between these three brain areas indicate that DLPFC's contribution is different than those from other areas because it was the only area we investigated that exhibited prominent power decreases. We found that DLPFC broad-band power decreased relative to baseline and, only for the theta-band, power decreased proportionally to memory load stronger this decrease was. Also, the extent of this power decrease was predictive of behavior on both a single-trial and subject-by-subject level. That is, people who were found to have a relatively bigger decrease in theta power were overall faster in accessing WM. In addition, we also found theta power changes in hippocampus and dACC. Strikingly, these were less pronounced and in the opposite direction compared to those in the DLPFC: in these areas theta power increased relative to baseline and as a function of load. Note that the power modulations we revealed were selective to the theta band only when we consider effects of load (Fig. 4). In contrast, the more general task versus baseline comparisons exhibited broadband effects (Fig. 5). This finding allows the hypothesis that theta-band power changes are specifically critical for WM maintenance.

Hippocampal theta has been extensively studied in both animals and humans, making its function relatively well understood (e.g., increases in theta power are associated with greater engagement and lead to better memory, see e.g. (Lin et al., 2017)). In contrast, the properties of theta in neocortex are less understood, making it unclear whether patterns similar to hippocampal theta modulation would be expected. Additionally, some studies show that theta power recorded on the scalp is inversely correlated with fMRI-BOLD changes (Michels et al., 2010a; Scheeringa et al., 2008, 2009). Here, we found that the patterns of theta power modulation were of opposite sign in DLPFC versus dACC and hippocampus, arguing for a differential role of theta in these two areas.

The load-related theta power changes in DLPFC that we found resemble those observed in DLPFC using both fMRI-BOLD as well as more direct measures of neural activity, but with opposite sign: BOLD or single-neuron studies reveal increases in activity as a function of memory load, whereas we here show a decrease in theta power as a function of memory load (Riley & Constantinidis, 2016; Veltman, Rombouts, & Dolan, 2003). One potential mechanism by which these differential effects can be explained is by considering the

hypothesis that low-frequency oscillations in neocortex are an index of excitability, with higher power indicative of less excitability. Related to this, it has indeed been hypothesized (Lisman & Jensen, 2013) that neocortical theta oscillations might have a role similar to cortical alpha, which is thought to index cortical excitability. Thus, if we assume that theta power indexes cortical excitability in ways similar to alpha power (Lisman & Jensen, 2013) and if we assume that less excitability is less metabolically demanding, then our results are in agreement with the literature on BOLD-fMRI studies of working memory in DLPFC.

Overall, our results support a distinction between how the medial and lateral parts of PFC support WM maintenance. Medial PFC shows increases in theta power (both in scalp EEG and intracranial recordings) and decrease in fMRI-BOLD activity as a function of load (Raichle & Raichle, 2001). On the other hand, the fMRI-BOLD signal increases in lateral parts of PFC during WM task performance, whereas the intracranial recordings described here as well as other existing studies (see Table 3) reveal decreases in theta power.

Several other intracranial studies considered changes of iEEG power during WM tasks (see Table 3 for summary). However, most of these focus on the task-related activity changes (compared to baseline activity) rather than prediction of behavior or load related changes (Howard, 2003; Meltzer et al., 2008; Raghavachari et al., 2001; Raghavachari & Lisman, 2006). An exception is the work of Meltzer et al (Meltzer et al., 2008), which compared the percentage of electrodes with positive or negative load-related power changes in patients performing a numerical Sternberg task between different regions of the brain. When comparing lateral (frontal, parietal) with medial (across entire medial wall) areas, they found that the percentage of electrodes with decreasing theta power as a function of load was larger in later compared to medial parts. While this coarse analysis does not allow conclusions specific to DLPFC, dACC, or hippocampus, this pattern is nevertheless compatible with that which we found here.

We previously studied the same task at the single-neuron level in dACC and hippocampus (but not DLPFC, where no neurons were recorded) (Kami ski et al., 2017). This previous work revealed that stimulus-selective neurons in the hippocampus maintained their activity throughout the maintenance period if their preferred stimulus was held in mind. The level of this persistent activity scaled inversely with load, with higher loads resulting in weaker persistent activity. In dACC, this previous study revealed non-stimulus selective maintenance units that maintained their elevated level of activity throughout the maintenance period. Single-neuron activity was thus elevated throughout the maintenance period in both areas, but the selectivity of this activity was different between brain areas. Here, we similarly found that power was changed relative to baseline throughout the baseline period and that such power changes scaled with load in different ways in different brain areas. It remains an open question how these single-neuron activity changes related to simultaneously recorded power changes and in particular how and whether the activity of single neurons in the human DLPFC is related to load during maintenance.

The theta power changes observed in our study in the DLPFC are different from those found in human EEG studies on frontal midline theta, which show that FMT power increase parametrically with memory load and/or the cognitive complexity of the task (Gärtner et al.,

2015; Hsieh & Ranganath, 2014; Onton et al., 2005). FMT theta is recorded from electrodes placed over the frontal midline (Anguera et al., 2013; Gärtner et al., 2015; Hsieh & Ranganath, 2014; Jensen & Tesche, 2002; Kami ski, Brzezicka, & Wróbel, 2011; Maurer et al., 2015), with a source that is frequently localized in the anterior cingulate (Hsieh & Ranganath, 2014; Onton et al., 2005). Surprisingly, we did not find load-related theta power changes in dACC that were similar to those observed with FMT. While we found that theta power increased during maintenance relative to baseline, the extent of this increase was not significantly related to memory load. One possibility is that parts of FMT are in fact volume conducted hippocampal theta. In addition, it is not known what the contribution of DLPFC is to FMT. Simultaneous scalp EEG (FMT) and intracranial dACC, hippocampal, and DLPFC recordings will be required to directly investigate this potential discrepancy, in particular in light of recent work that indicates that LFP and EEG power can be disassociated in some instances (Musall, Von Pföstl, Rauch, Logothetis, & Whittingstall, 2014).

Our results are also of relevance to a recently proposed model on the interplay between hippocampus and neocortex during episodic memory formation (Parish, Hanslmayr, & Bowman, 2018). This model proposes that lower frequency oscillations (alpha in their case) have different roles in the hippocampus and cortex (Parish et al., 2018). The reasoning for this rests on two assumptions. First, neurons in neocortex need to 'break out' of an ongoing oscillation to represent a stimulus, which is achieved by desynchronization. Second, firing of hippocampal neurons in synchrony with ongoing theta oscillations facilitates formation of memories (i.e., theta synchronizes). Accordingly, successful memory formation is marked by both reduced neocortical alpha and increased hippocampal theta. While originally proposed for episodic memory, our data suggests that this mode of operation might also be valid for WM, with theta serving two different roles – desynchronizing activity of neurons in neocortex (DLPFC) and synchronizing in hippocampus during WM maintenance. A key caveat is, however, that here we did not quantify synchronization. Rather, we measured only power changes, which might be due to changes in synchronization but can also result from other type of activity changes. Answering this question conclusively will require quantifying synchrony between pairs of neurons recorded in DLFPC, which is data that we do not have access to here.

An important question that our results raise is how power decreases in a given area can be functionally beneficial (as ours were, as demonstrated by the correlation with behavior). With respect to theta, this question is little studied, since most of the literature so far focused on power increases and their functional role. One hypothesis is that neurons that code for particular stimuli form small ensembles and synchronize with each other at different (mostly higher than theta) frequencies , resulting in decreased theta power for higher loads. Another hypothesis is that there are several independent local theta generators (i.e. here one for hippocampus, one for DLPFC) that change differently as a function of load (Raghavachari et al., 2009)). Note that in contrast to theta, beta-power reductions and the resulting desynchronization are prominent phenomena in the motor system that are well understood and which are necessary for properly releasing a motor movement (Crowell et al., 2012). So a third hypothesis is that in DLPFC theta acts akin to beta in the motor cortex.

What function does a WM theta power decrease in the DLPFC index? WM involves several theoretical constructs (see e.g.(Conway, A., Jarrold, C., Kane, M., & Miyake, 2008)), including one related to cognitive control and another related to storage itself. Our task only concerns storage, but no active manipulations during maintenance. In addition, we observe prominent load-related changes in neural activity. For this reason, we hypothesize that the theta power decrease we found in DLPFC are a reflection of the storage component of WM. A key question that remains to be answered is what the relationship is between these power decreases and the activity of individual neurons in DLPFC. One hypothesis is that as a result of reduced power, synchrony between pairs of neurons in DLPFC would decrease, thereby allowing more independent storage of different items. Single-neuron recordings in DLPFC will be required to answer this question. Of relevance, recent work (Vries, Driel, Karacaoglu, & Olivers, 2018) suggests that frontal areas might use low-frequency theta to drive changes in more posterior areas and thus the role of prefrontal cortex might be crucial for storage only indirectly, because the but storage as such takes places elsewhere.

Our results seem also to be contradictory to the "theta gating" hypothesis (Raghavachari et al., 2001), which proposes that the amplitude of theta oscillations increases at the start of a cognitive task (e.g. Sternberg task), than continues to be elevated through all phases of the trial, including the delay period, and decreases sharply at the end of the maintaining period. However, this effect is not apparent on all electrodes analyzed (Raghavachari et al., 2001). Rather, its presence is conditional on where an electrode was placed, with some electrodes showing the opposite pattern (Raghavachari et al., 2001). This is compatible with our observation, which shows that the pattern of change depends on where in the cortex theta is recorded from. It might be possible that neocortical areas are more likely to show theta decreases compared to allocortex (hippocampus, dACC). Such thinking is supported by some animal studies. For example, studies utilizing macaques performing a visual working memory task (Kornblith, Buschman, & Miller, 2016) have revealed load-related decrease in low-frequency power.

Is the activity in DLPFC that we measure here related to preparatory motor activity, thereby explaining the ability of theta power in DLFPC to predict response speed? To exclude this possibility, we only included data during the maintenance period, excluding data from the probe period in our analysis. In addition, the maintenance period length was unpredictable, making it impossible for a subject to know when the probe image was displayed. For this reason, we do not believe that the theta power reduction we observed in DLPFC is a reflection of motor preparation.

Our results show that task- and load-related theta power changes in the DLPFC predict an individual person's accuracy and speed during a WM task. Note, however, that due to the limited size of our subject pool (13 subjects), the statistical power to explain individual differences in this dataset is limited and larger studies are needed to confirm these putative individual differences. We found this relationship on two levels: intra- and inter-individual. We saw that trials characterized by a bigger drop in theta power during maintenance compared to the baseline were more likely to end with the patient producing a correct response, with a faster RT. We also found that subjects exhibiting a greater amount of theta decrease in the DLPFC had faster response times. These results support the view that

DLPFC theta power changes explain individual differences in RT in a working memory task. WM ability varies greatly between individuals (Shipstead et al., 2016; Unsworth & Engle, 2006, 2007), with important consequences for a person's overall cognitive function. It is thus important to discover features of WM that differ between individuals. Here, we found such a relationship in DLPFC. This extends previous work using scalp EEG, in which we found a similar relationship for FMT (Zakrzewska & Brzezicka, 2014). Together, these data indicate that theta power in DLPFC is a metric that may help explain individual differences in WM and may be used as a neurophysiological indicator of WM efficiency.

References

Altamura M, Elvevåg B, Blasi G, Bertolino A, Callicott JH, Weinberger DR, … Goldberg TE (2007). Dissociating the effects of Sternberg working memory demands in prefrontal cortex. Psychiatry Research - Neuroimaging, 154(2), 103–114. 10.1016/j.pscychresns.2006.08.002

Anguera JA, Boccanfuso J, Rintoul JL, Al-Hashimi O, Faraji F, Janowich J, … Gazzaley A (2013). Video game training enhances cognitive control in older adults. Nature, 501(7465), 97–101. 10.1038/nature12486 [PubMed: 24005416]

Asada H, Fukuda Y, Tsunoda S, Yamaguchi M, & Tonoike M (1999). Frontal midline theta rhythms reflect alternative activation of prefrontal cortex and anterior cingulate cortex in humans. Neuroscience Letters, 274(1), 29–32. Retrieved from http://www.ncbi.nlm.nih.gov/pubmed/10530512 [PubMed: 10530512]

Avants B, Duda JT, Kim J, Zhang H, Pluta J, Gee JC, & Whyte J (2008). Multivariate Analysis of Structural and Diffusion Imaging in Traumatic Brain Injury. Academic Radiology, 15(11), 1360–1375. 10.1016/j.acra.2008.07.007 [PubMed: 18995188]

Axmacher N, Henseler MM, Jensen O, Weinreich I, Elger CE, & Fell J (2010). Cross-frequency coupling supports multi-item working memory in the human hippocampus. Proc Natl Acad Sci U S A, 107(7), 3228–3233. [PubMed: 20133762]

Baddeley A (2010). Working memory. Current Biology: CB, 20(4), R136–40. 10.1016/j.cub.2009.12.014 [PubMed: 20178752]

Bagherzadeh Y, Khorrami A, Zarrindast MR, Shariat SV, & Pantazis D (2016). Repetitive transcranial magnetic stimulation of the dorsolateral prefrontal cortex enhances working memory. Experimental Brain Research, 234(7), 1807–1818. 10.1007/s00221-016-4580-1 [PubMed: 26884132]

Bähner F, Demanuele C, Schweiger J, Gerchen MF, Zamoscik V, Ueltzhöffer K, … Meyer-Lindenberg A (2015). Hippocampal-dorsolateral prefrontal coupling as a species-conserved cognitive mechanism: A human translational imaging study. Neuropsychopharmacology, 40(7), 1674–1681. 10.1038/npp.2015.13 [PubMed: 25578799]

Barbey AK, Koenigs N, & Grafman J (2013). Dorsolateral Prefrontal Contributions to Human Working Memory. Cortex, 49(5), 1195–1205. 10.1016/j.cortex.2012.05.022.Dorsolateral [PubMed: 22789779]

Conway A, Jarrold C, Kane M, & Miyake A (Ed.). (2008). Variation in working memory. Oxford University Press.

Crowell AL, Ryapolova-webb ES, Ostrem JL, Galifianakis NB, Shimamoto S, Lim DA, & Starr PA (2012). Oscillations in sensorimotor cortex in movement disorders: an electrocorticography study. 10.1093/brain/awr332

Curtis CE, & D'Esposito M (2003). Persistent activity in the prefrontal cortex during working memory. Trends in Cognitive Sciences, 7(9), 415–423. 10.1016/S1364-6613(03)00197-9 [PubMed: 12963473]

Delorme A, & Makeig S (2004). EEGLAB: an open source toolbox for analysis of single-trial EEG dynamics including independent component analysis. J Neurosci Meth, 134(1), 9–21.

Finn AS, Sheridan MA, Kam CLH, Hinshaw S, & D'Esposito M (2010). Longitudinal Evidence for Functional Specialization of the Neural Circuit Supporting Working Memory in the Human Brain.

Journal of Neuroscience, 30(33), 11062–11067. 10.1523/JNEUROSCI.6266-092010. [PubMed: 20720113]

Funahashi S (2017). Working memory in the prefrontal cortex. Brain Sciences, 7(5). 10.3390/brainsci7050049

Fuster JM (1973). Unit activity in prefrontal cortex during delayed-response performance: neuronal correlates of transient memory. Journal of Neurophysiology, 36(1), 61–78. 10.1152/jn.1973.36.1.61 [PubMed: 4196203]

Fuster JM, & Alexander GE (1971). Neuron Activity Related to Short-Term Memory. Science, 173(3997), 652–654. 10.1126/science.173.3997.652 [PubMed: 4998337]

Gärtner M, Grimm S, & Bajbouj M (2015). Frontal midline theta oscillations during mental arithmetic: effects of stress. Frontiers in Behavioral Neuroscience, 9(April), 1–8. 10.3389/fnbeh.2015.00096 [PubMed: 25653603]

Goldman-Rakic PS (1995). Cellular basis of working memory. Neuron, 14(3), 477–485. 10.1016/0896-6273(95)90304-6 [PubMed: 7695894]

Helfrich RF, & Knight RT (2016). Oscillatory Dynamics of Prefrontal Cognitive Control. Trends in Cognitive Sciences, 20(12), 916–930. 10.1016/j.tics.2016.09.007 [PubMed: 27743685]

Howard MW (2003). Gamma Oscillations Correlate with Working Memory Load in Humans. Cerebral Cortex, 13(12), 1369–1374. 10.1093/cercor/bhg084 [PubMed: 14615302]

Hsieh LT, & Ranganath C (2014). Frontal midline theta oscillations during working memory maintenance and episodic encoding and retrieval. NeuroImage, 85, 721–729. 10.1016/j.neuroimage.2013.08.003 [PubMed: 23933041]

Jansma JM, Ramsey NF, De Zwart JA, Van Gelderen P, & Duyn JH (2007). fMRI study of effort and information processing in a working memory task. Human Brain Mapping, 28(5), 431–440. 10.1002/hbm.20297 [PubMed: 17133397]

Jensen O, & Tesche CD (2002). Frontal theta activity in humans increases with memory load in a working memory task. Eur J Neurosci, 15(8), 1395–1399. [PubMed: 11994134]

Kami ski J, Brzezicka A, & Wróbel A (2011). Short-term memory capacity (7 ± 2) predicted by theta to gamma cycle length ratio. Neurobiol Learn Mem, 95(1), 19–23. 10.1016/j.nlm.2010.10.001 [PubMed: 20951219]

Kami ski J, Sullivan S, Chung JM, Ross IB, Mamelak AN, & Rutishauser U (2017). Persistently active neurons in human medial frontal and medial temporal lobe support working memory. Nature Neuroscience, 20(4), 590–601. 10.1038/nn.4509 [PubMed: 28218914]

Kornblith S, Buschman TJ, & Miller EK (2016). Stimulus Load and Oscillatory Activity in Higher Cortex, (August 2015), 3772–3784. 10.1093/cercor/bhv182

Lara AH, & Wallis JD (2015). The Role of Prefrontal Cortex in Working Memory: A Mini Review. Frontiers in Systems Neuroscience, 9(December), 1–7. 10.3389/fnsys.2015.00173

Lee H, Simpson GV, Logothetis NK, & Rainer G (2005). Phase locking of single neuron activity to theta oscillations during working memory in monkey extrastriate visual cortex. Neuron, 45(1), 147–156. 10.1016/j.neuron.2004.12.025 [PubMed: 15629709]

Lega BC, Jacobs J, & Kahana M (2012). Human hippocampal theta oscillations and the formation of episodic memories. Hippocampus, 22(4), 748–761. 10.1002/hipo.20937 [PubMed: 21538660]

Lenartowicz A, & McIntosh AR (2005). The role of anterior cingulate cortex in working memory is shaped by functional connectivity. Journal of Cognitive Neuroscience, 17(7), 1026–1042. 10.1162/0898929054475127 [PubMed: 16102235]

Lin JJ, Rugg MD, Das S, Stein J, Rizzuto DS, Kahana MJ, & Lega BC (2017). Theta band power increases in the posterior hippocampus predict successful episodic memory encoding in humans. Hippocampus, 27(10), 1040–1053. 10.1002/hipo.22751 [PubMed: 28608960]

Lisman JE, & Jensen O (2013). The Theta-Gamma Neural Code. Neuron, 77(6), 1002–1016. 10.1016/j.neuron.2013.03.007 [PubMed: 23522038]

Manoach DS, Schlaug G, Siewert B, Darby DG, Bly BM, Benfield a, … Warach S (1997). Prefrontal cortex fMRI signal changes are correlated with working memory load. Neuroreport, 8(2), 545–549. 10.1097/00001756-199701200-00033 [PubMed: 9080445]

Maris E, & Oostenveld R (2007). Nonparametric statistical testing of EEG- and MEG-data. Journal of Neuroscience Methods, 164(1), 177–190. 10.1016/j.jneumeth.2007.03.024 [PubMed: 17517438]

Maurer U, Brem S, Liechti M, Maurizio S, Michels L, & Brandeis D (2015). Frontal midline theta reflects individual task performance in a working memory task. Brain Topography, 28(1), 127–134. 10.1007/s10548-014-0361-y [PubMed: 24687327]

Meltzer JA, Negishi M, Mayes LC, & Constable RT (2007). Individual differences in EEG theta and alpha dynamics during working memory correlate with fMRI responses across subjects. Clinical Neurophysiology: Official Journal of the International Federation of Clinical Neurophysiology, 118(11), 2419–2436. 10.1016/j.clinph.2007.07.023 [PubMed: 17900976]

Meltzer JA, Zaveri HP, Goncharova II, Distasio MM, Papademetris X, Spencer SS, … Constable RT (2008). Effects of working memory load on oscillatory power in human intracranial EEG. Cerebral Cortex, 18(8), 1843–1855. 10.1093/cercor/bhm213 [PubMed: 18056698]

Michels L, Bucher K, Lüchinger R, Klaver P, Martin E, Jeanmonod D, & Brandeis D (2010a). Simultaneous EEG-fMRI during a working memory task: modulations in low and high frequency bands. PloS One, 5(4), e10298 10.1371/journal.pone.0010298 [PubMed: 20421978]

Michels L, Bucher K, Lüchinger R, Klaver P, Martin E, Jeanmonod D, & Brandeis D (2010b). Simultaneous EEG-fMRI during a working memory task: Modulations in low and high frequency bands. PLoS ONE, 5(4). 10.1371/journal.pone.0010298

Minxha J, Mamelak AN, & Rutishauser U (2018). Surgical and Electrophysiological Techniques for Single-Neuron Recordings in Human Epilepsy Patients In Extracellular Recording Approaches. (pp. 267–293). New York: Humana Press.

Minxha J, Mosher C, Morrow JK, Mamelak AN, Adolphs R, Gothard KM, & Rutishauser U (2017). Fixations Gate Species-Specific Responses to Free Viewing of Faces in the Human and Macaque Amygdala. Cell Reports, 18(4), 878–891. 10.1016/j.celrep.2016.12.083 [PubMed: 28122239]

Mitchell DJ, McNaughton N, Flanagan D, & Kirk IJ (2008). Frontal-midline theta from the perspective of hippocampal "theta". Prog Neurobiol, 86(3), 156–185. 10.1016/j.pneurobio.2008.09.005 [PubMed: 18824212]

Morgan HM, Jackson MC, Van Koningsbruggen MG, Shapiro KL, & Linden DEJ (2013). Frontal and parietal theta burst TMS impairs working memory for visual-spatial conjunctions. Brain Stimulation, 6(2), 122–129. 10.1016/j.brs.2012.03.001 [PubMed: 22483548]

Musall S, Von Pföstl V, Rauch A, Logothetis NK, & Whittingstall K (2014). Effects of neural synchrony on surface EEG. Cerebral Cortex, 24(4), 1045–1053. 10.1093/cercor/bhs389 [PubMed: 23236202]

Mylius V, Ayache SS, Ahdab R, Farhat WH, Zouari HG, Belke M, … Lefaucheur JP (2013). Definition of DLPFC and M1 according to anatomical landmarks for navigated brain stimulation: Inter-rater reliability, accuracy, and influence of gender and age. NeuroImage, 78, 224–232. 10.1016/j.neuroimage.2013.03.061 [PubMed: 23567888]

Nouwens S, Groen MA, & Verhoeven L (2017). How working memory relates to children's reading comprehension: the importance of domain-specificity in storage and processing. Reading and Writing, 30(1), 105–120. 10.1007/s11145-016-9665-5 [PubMed: 28163387]

Onton J, Delorme A, & Makeig S (2005). Frontal midline EEG dynamics during working memory. NeuroImage, 27(2), 341–356. 10.1016/j.neuroimage.2005.04.014 [PubMed: 15927487]

Parish G, Hanslmayr S, & Bowman H (2018). The Sync/deSync model: How a synchronized hippocampus and a de-synchronized neocortex code memories. The Journal of Neuroscience, 38(14), 2561–17. 10.1523/JNEUROSCI.2561-17.2018

Raghavachari S, Kahana MJ, Rizzuto DS, Caplan JB, Kirschen MP, Bourgeois B, … Lisman JE (2001). Gating of human theta oscillations by a working memory task. The Journal of Neuroscience: The Official Journal of the Society for Neuroscience, 21(9), 3175–3183. https://doi.org/21/9/3175 [pii]

Raghavachari S, & Lisman J (2006). Theta oscillations in human cortex during a working-memory task: evidence for local generators. J Neurophysiol, 1630–1638. 10.1152/jn.00409.2005. [PubMed: 16207788]

Raghavachari S, Lisman JE, Tully M, Madsen JR, Bromfield EB, Kahana J, & Kahana MJ (2009). Theta Oscillations in Human Cortex During a Working-Memory Task: Evidence for Local Generators. Journal of Neurophysiology, 1630–1638. 10.1152/jn.00409.2005

Raichle ME, & Raichle ME (2001). Searching for a baseline: Functional imaging and the resting human brain. Nature Reviews Neuroscience, 2(10), 685–694. 10.1038/35094500 [PubMed: 11584306]

Rajkowska G, & Goldman-Rakic P. s. (1995). Cytoarchitectonic definition of prefrontal areas in the normal human cortex: I. Remapping of areas 9 and 46 using quantitative criteria. Cerebral Cortex, 5(4), 307–322. [PubMed: 7580124]

Reuter M, Rosas HD, & Fischl B (2010). Highly accurate inverse consistent registration: A robust approach. NeuroImage, 53(4), 1181–1196. 10.1016/j.neuroimage.2010.07.020 [PubMed: 20637289]

Riley MR, & Constantinidis C (2016). Role of Prefrontal Persistent Activity in Working Memory. Frontiers in Systems Neuroscience, 9(January), 1–14. 10.3389/fnsys.2015.00181

Rottschy C, Langner R, Dogan I, Reetz K, Laird AR, Schulz JB, … Eickhoff SB (2012). Modelling neural correlates of working memory: A coordinate-based meta-analysis. NeuroImage, 60(1), 830–846. 10.1016/j.neuroimage.2011.11.050 [PubMed: 22178808]

Roux F, & Uhlhaas PJ (2014). Working memory and neural oscillations: Alpha-gamma versus theta-gamma codes for distinct WM information? Trends in Cognitive Sciences, 18(1), 16–25. 10.1016/j.tics.2013.10.010 [PubMed: 24268290]

Scheeringa R, Bastiaansen MCM, Petersson KM, Oostenveld R, Norris DG, & Hagoort P (2008). Frontal theta EEG activity correlates negatively with the default mode network in resting state. International Journal of Psychophysiology: Official Journal of the International Organization of Psychophysiology, 67(3), 242–251. 10.1016/j.ijpsycho.2007.05.017

Scheeringa R, Petersson KM, Oostenveld R, Norris DG, Hagoort P, & Bastiaansen MCM (2009). Trial-by-trial coupling between EEG and BOLD identifies networks related to alpha and theta EEG power increases during working memory maintenance. NeuroImage, 44(3), 1224–1238. 10.1016/j.neuroimage.2008.08.041 [PubMed: 18840533]

Schicktanz N, Fastenrath M, Milnik A, Spalek K, Auschra B, Nyffeler T, … Schwegler K (2015). Continuous theta burst stimulation over the left dorsolateral prefrontal cortex decreases medium load working memory performance in healthy humans. PLoS ONE, 10(3), 1–10. 10.1371/journal.pone.0120640

Ségonne F, Dale AM, Busa E, Glessner M, Salat D, Hahn HK, & Fischl B (2004). A hybrid approach to the skull stripping problem in MRI. NeuroImage, 22(3), 1060–1075. 10.1016/j.neuroimage.2004.03.032 [PubMed: 15219578]

Shipstead Z, Harrison TL, & Engle RW (2016). Working Memory Capacity and Fluid Intelligence: Maintenance and Disengagement. Perspectives on Psychological Science, 11(6), 771–799. 10.1177/1745691616650647 [PubMed: 27899724]

Spellman T, Rigotti M, Ahmari SE, Fusi S, Joseph A, Gordon JA, … Program N (2015). Hippocampal-prefrontal input supports spatial encoding in working memory. Nature, 522(7556), 309–314. 10.1038/nature14445.Hippocampal-prefrontal [PubMed: 26053122]

Sternberg S (1966). High speed scanning in human memory. Science, 153(3736), 652–654. [PubMed: 5939936]

Tesche CD, & Karhu J (2000). Theta oscillations index human hippocampal activation during a working memory task. Proceedings of the National Academy of Sciences, 97(2), 919–924. 10.1073/pnas.97.2.919

The MathWorks. (2015). MATLAB 2015a. Natick.

Tsujimoto T, Shimazu H, Isomura Y, & Sasaki K (2010). Theta Oscillations in Primate Prefrontal and Anterior Cingulate Cortices in Forewarned Reaction Time Tasks. Journal of Neurophysiology, 103(2), 827–843. 10.1152/jn.00358.2009 [PubMed: 20007502]

Tyszka JM, & Pauli WM (2016). A high resolution in vivo MRI atlas of the adult human amygdaloid complex. Human Brain Mapping, 37(11), 3979–3998. [PubMed: 27354150]

Unsworth N, & Engle RW (2006). Simple and complex memory spans and their relation to fluid abilities: Evidence from list-length effects. Journal of Memory and Language, 54(1), 68–80. 10.1016/j.jml.2005.06.003

Unsworth N, & Engle RW (2007). The nature of individual differences in working memory capacity: Active maintenance in primary memory and controlled search from secondary memory. Psychological Review, 114(1), 104–132. 10.1037/0033-295X.114.1.104 [PubMed: 17227183]

van Vugt MK, Schulze-Bonhage A, Litt B, Brandt A & Kahana MJ (2010). Hippocampal gamma oscillations increase with memory load. Journal of Neuroscience, 30(7), 2694–2699. [PubMed: 20164353]

Veltman DJ, Rombouts SARB, & Dolan RJ (2003). Maintenance versus manipulation in verbal working memory revisited: An fMRI study. NeuroImage, 18(2), 247–256. 10.1016/S1053-8119(02)00049-6 [PubMed: 12595179]

De Vries IEJ, Van Driel J, Karacaoglu M, & Olivers CNL (2018). Priority Switches in Visual Working Memory are Supported by Frontal Delta and Posterior Alpha Interactions, (November), 4090–4104. 10.1093/cercor/bhy223

Wang X-J (2010). Neurophysiological and Computational Principles of Cortical Rhythms in Cognition. Physiological Reviews, 90(3), 1195–1268. 10.1152/physrev.00035.2008 [PubMed: 20664082]

Wiley J, & Jarosz AF (2012). How working memory capacity affects problem solving. In Psychology of learning and motivation, Vol. 56 (pp. 185–227).

Wisniewski MG, Thompson ER, Iyer N, Estepp JR, Goder-Reiser MN, & Sullivan SC (2015). Frontal midline?? power as an index of listening effort. NeuroReport, 26(2), 94–99. 10.1097/WNR.0000000000000306 [PubMed: 25536119]

Womelsdorf T, Johnston K, Vinck M, & Everling S (2010). Theta-activity in anterior cingulate cortex predicts task rules and their adjustments following errors. Proceedings of the National Academy of Sciences of the United States of America, 107(11), 5248–5253. 10.1073/pnas.0906194107 [PubMed: 20194767]

Yoon T, Okada J, Jung M, & Kim J (2008). Prefrontal cortex and hippocampus subserve different components of working memory in rats. Learning & Memory, 15, 97–105. 10.1101/lm.850808.to-sample

Zakrzewska MZ, & Brzezicka A (2014). Working memory capacity as a moderator of load-related frontal midline theta variability in Sternberg task. Frontiers in Human Neuroscience, 8(JUNE). 10.3389/fnhum.2014.00399
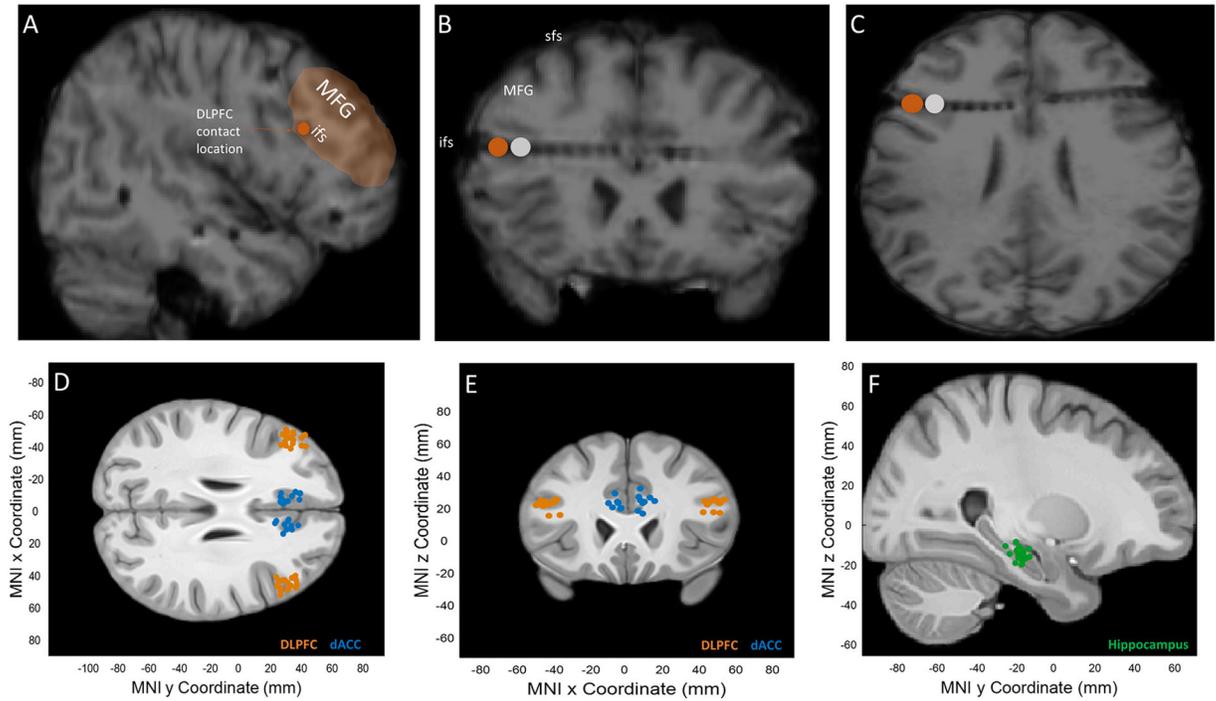
Figure 1. Electrode localization.
(A-C) Illustration of DLPFC electrode in one individual brain (P37CS). Abbreviations: medial frontal gyrus (MFG); inferior frontal sulcus (ifs); superior frontal sulcus (sfs). Orange shows the active contact, grey the reference contact used for analysis. (D-F) Summary of all recording locations, shown in Montreal Neurological Institute's MNI152 space displayed superimposed on the California Institute of Technology's CIT168 T1w brain atlas (Tyszka & Pauli, 2016). Recording locations are indicated by different colors (D, E: orange - DLPFC; blue - dACC; F: green - Hippocampus).
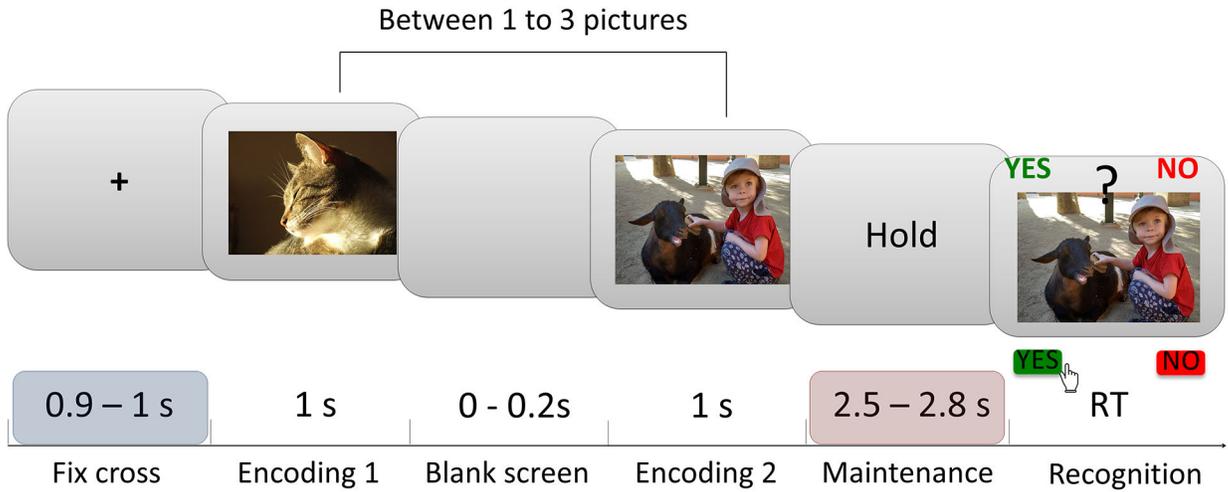
Figure 2. The task.

Top: example of the screens presented to the subjects during an example trial (here with memory load 2). Bottom: the duration for which each screen is shown. Each trial started with an encoding phase, during which between 1–3 sequentially presented pictures were shown. This was followed by the maintenance (delay) period. Finally, after the delay, a probe image was shown. Subjects were asked to indicate whether the probe was or was not shown during the encoding period that immediately preceded the probe. All analysis shown in this paper was performed during the maintenance and baseline periods (red and blue, respectively).
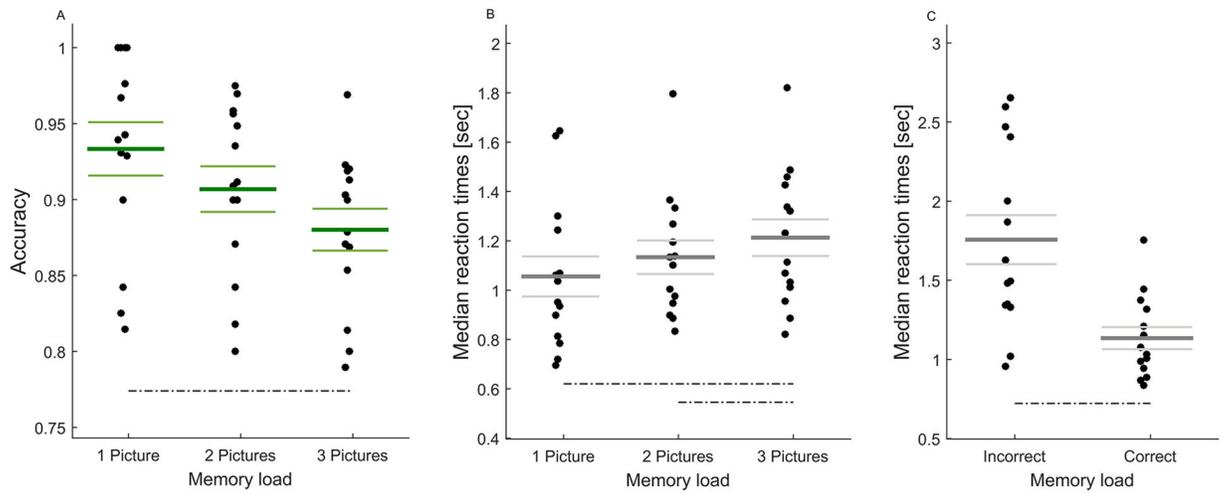
Figure 3. Behavioral results.

(A) Accuracy decreased as a function of load. (B) Reaction time increased as a function of load. (C) Reaction time differed significantly between correct and incorrect trials. Panel C only includes data from load 3. Each dot shows one session. Dotted lines indicate significant pairwise differences at p<.05.
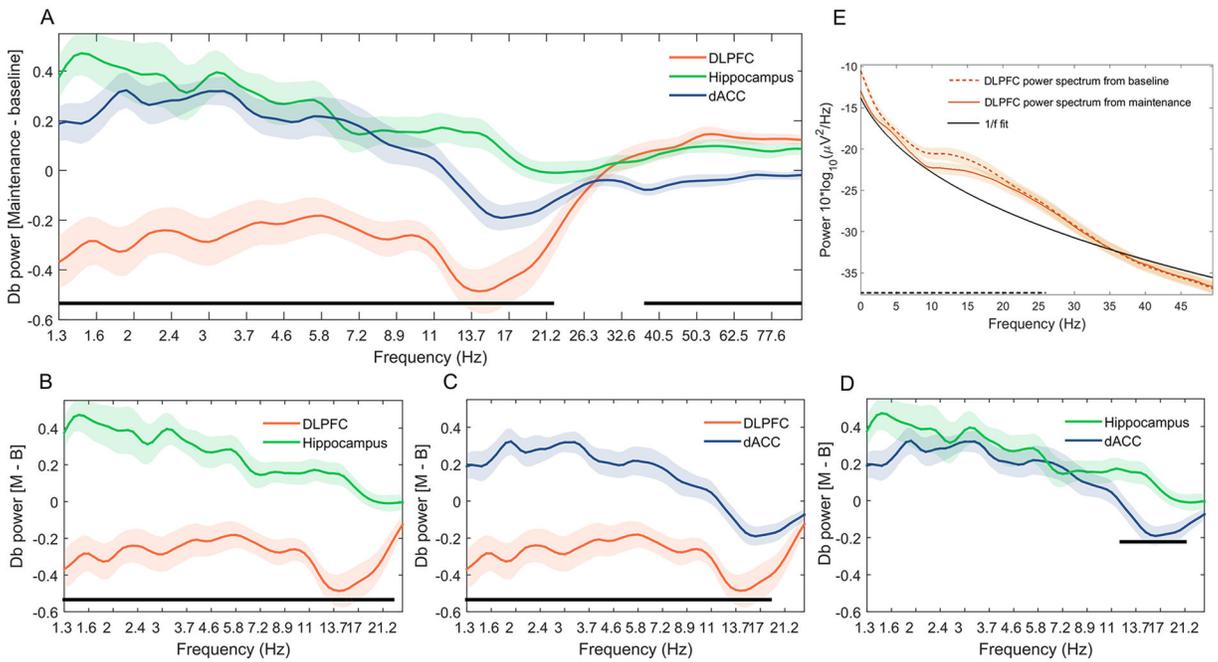
Figure 4. Broad-band power changes relative to baseline during maintenance.
Spectral comparisons between task (maintenance period) and baseline for DLPFC, hippocampus and dACC showing contrasting effects between neocortex (DLPFC) and allocortex (hippocampus and dACC). Plots show averaged power during maintenance in units of dB relative to baseline across all electrodes in a given brain area. (A) Power as a function of frequency for DLPFC, dACC, and hippocampus. Significance indicated is the result of a 1×3 ANOVA at p<0.05. (B-D) Pairwise differences between brain areas. Significance indicated is computed using post hoc tests (permuted t-tests). All significant data points marked as a black line are significant at p<0.05 and corrected for multiple comparisons using a cluster-based approach (Maris & Oostenveld, 2007). In DLPFC the difference was negative (decrease in power during maintenance relative to the baseline) and most pronounced at 2Hz (p=.0012), 3Hz (p=.0062) and then 6.5 up to 20 Hz (p=.0012). In hippocampus the difference was positive (increase in power during maintenance compared to the baseline period) and most pronounced between 2.8 – 6.3 Hz (p=.0012). In dACC the difference was positive in lower bands (increase in power during maintenance compared to the baseline period, between 2–6.5 Hz, p=.0012) and negative in higher bands (decrease in power during maintenance relative to the baseline, between 15–22 Hz, p=.0012). (E) Raw power spectra from maintenance and baseline periods of the task for DLPFC. The black dotted line denotes statistically significance of the difference between the expected 1/f background and the measured DLPFC power spectra (1×3 permuted repeated measures ANOVA corrected for multiple comparisons using cluster-based approach).
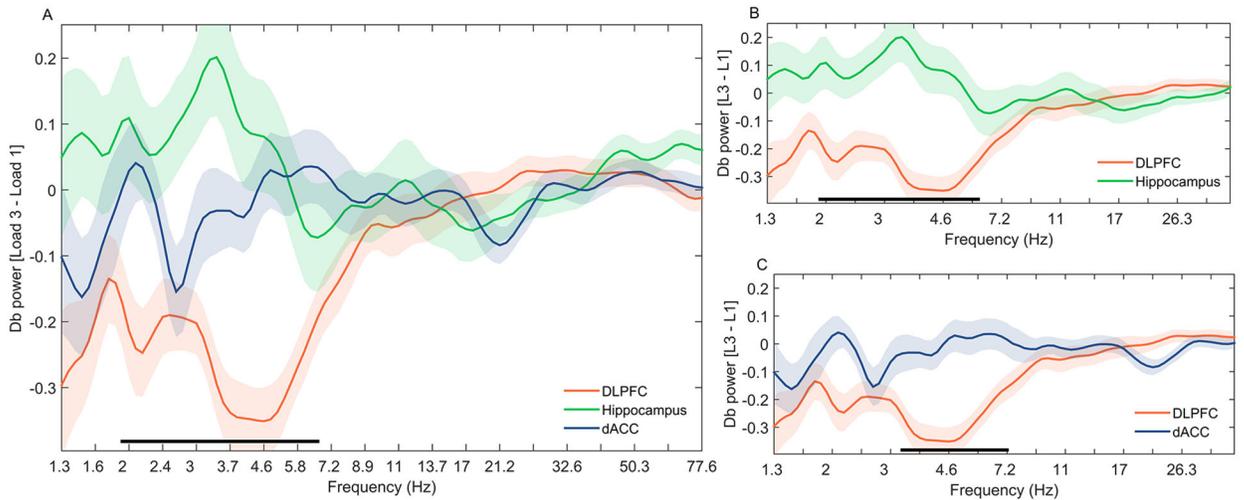
Figure 5. Theta-band power is modulated by load during maintenance.
(A) Differences in power between load 3 and 1, averaged across all electrodes located in a given brain area (correct trials only). Each line represents the difference in power between trials with high (3 pictures in memory) and low memory load (1 picture in memory). Black line indicates significant differences between the three areas as indicated by a 1×3 ANOVA at p<0.05. (B-C) Pairwise comparisons between DLPFC and hippocampus (B) and DLPFC and dACC (C). Black line indicates significant differences derived from post hoc tests at p<0.05 (permuted t-tests for independent samples). The comparison between hippocampus and dACC did not revealed statistically significant differences and is not shown. All comparisons were performed with correction for multiple comparisons using cluster based approach (Maris & Oostenveld, 2007).
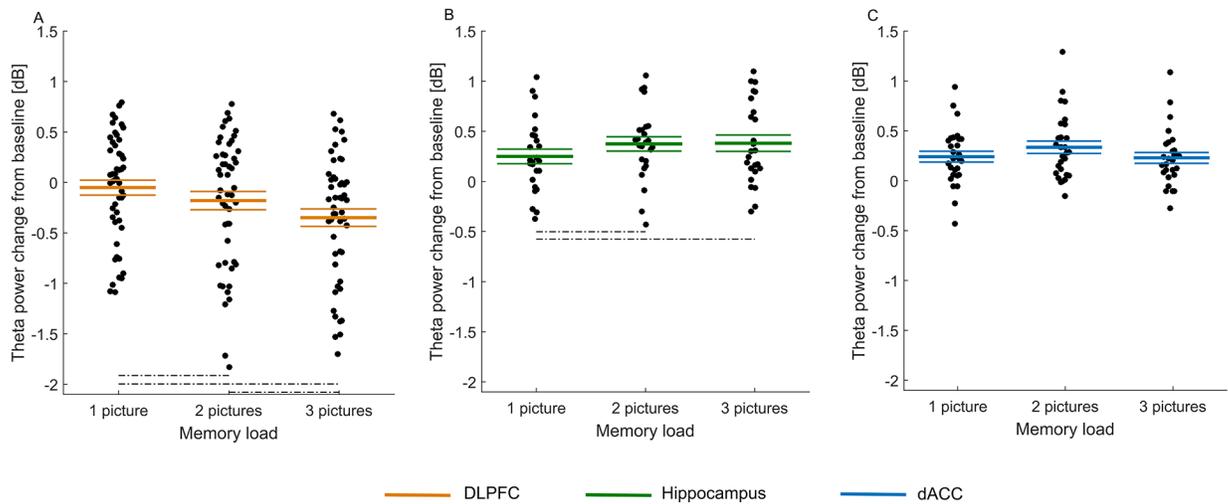
Figure. 6. Theta (3–6 Hz) power modulation by memory load in DLPFC, hippocampus and dACC.

Changes of theta power as a function of load quantified at the single-electrode level (each dot is an electrode). (A) DLFPC theta power decreases significantly as a function of load (see text for statistics). (B) In hippocampus, theta power increased significantly as a function of load, but the strength of this modulation was significantly weaker compared to that in DLPFC (see A). (C) In dACC, we found no significant effect of memory load on theta power (but note that for each load, power is significantly stronger then baseline) dashed lines denote statistically significant differences at $p < .05$.
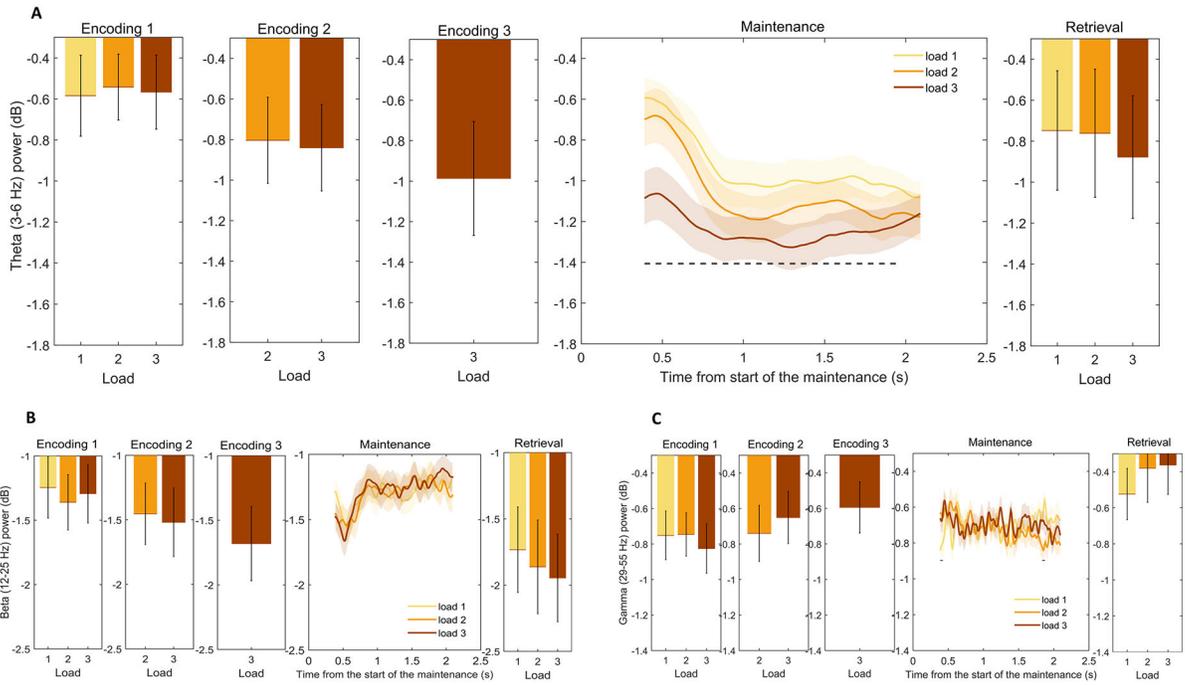
Figure 7. Theta, beta and gamma power time courses throughout the task in DLPFC.
Power changes as a function of time for (A) theta (B) beta and (C) gamma band. Power was calculated with the Morlet continuous wavelet transform (CWT; 16 scales per octave, minimum period to analyze was set to 0.01 and maximum period was set to 0.8) as implemented in WAVOS (Wavos 2.3.1) and then transformed to decibels relative to the average power during the baseline period. To avoid contamination from visual transients we only used the time period starting at 400–2100 ms following the start of the maintenance period to compute power. For the same reason, to calculate the power in the encoding and retrieval periods (bars) we used a time window of 200–1000ms following image onset. Note that significant load differences during maintenance are only apparent in the theta band (A). All p values are based on permuted repeated measures ANOVA corrected for multiple comparisons using a cluster-based approach (dashed line denotes at which time points differences are statistically significant).

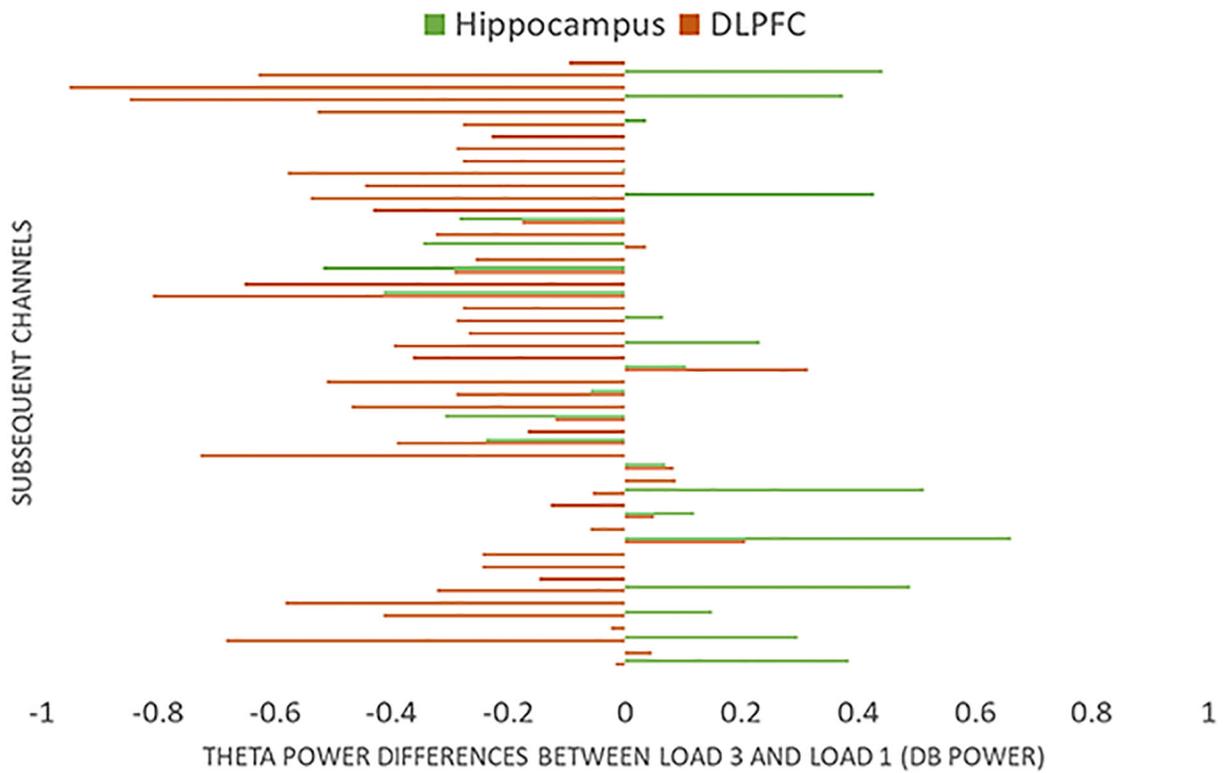**Figure 8. Theta power modulation by memory load on individual electrodes from DLPFC and hippocampus.**

Illustration of the modulation of theta power as a function of load individually for all electrodes recorded in DLPFC and hippocampus, ordered as recorded (from top to bottom, oldest at top). Of the 23 hippocampal channels, 12 showed increases. Of the 48 DLPFC channels, 34 showed decreases.
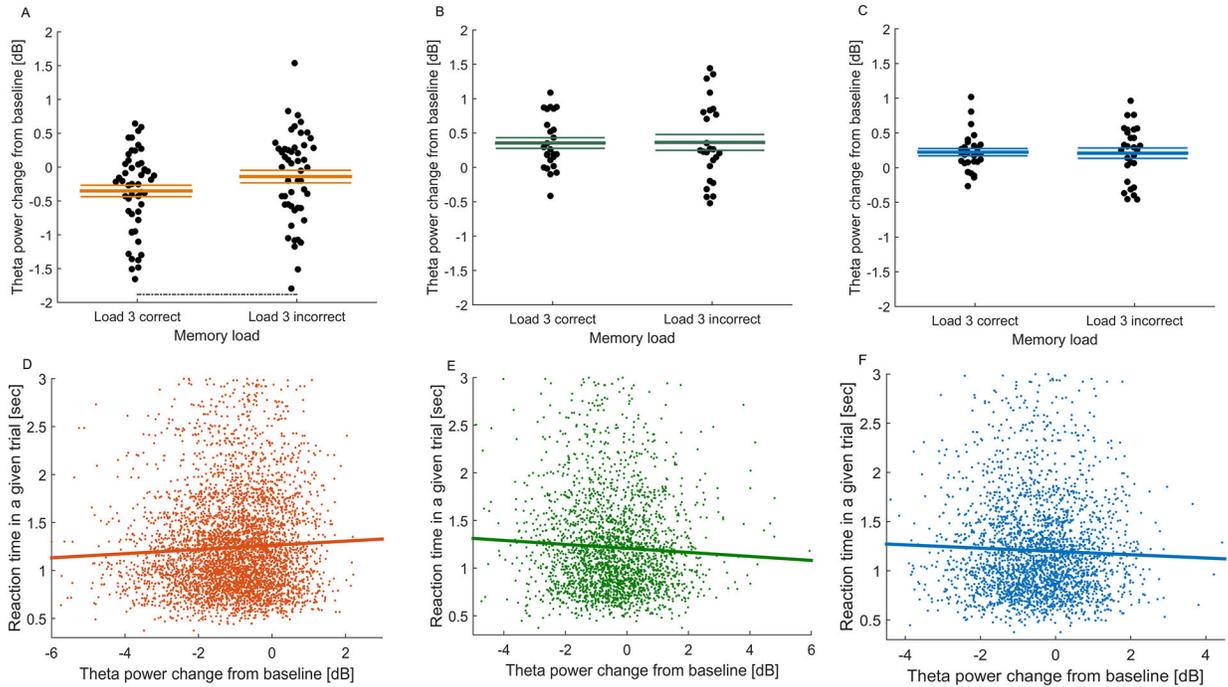
Figure 9. Theta power as a predictor of task performance.
(A-C) Comparison of theta power change from baseline in correct versus incorrect trials (in memory load 3 trials only) for DLPFC (A), Hippocampus (B) and dACC (C) [each dot is an electrode, dashed line denotes statistically significant difference at p<.05]. (D-F) The relationship between RT and theta power change from baseline for all trials in DLPFC (D), Hippocampus (E) and dACC (F). Each dot is a trial. All relationships were statistically significant, post hoc to the main analysis (linear mixed effects model with RT and brain area as fixed factors, channels as random factor and theta power as the dependent variable) were as follows: DLPFC, $r = 0.052$, $p = 3.2949e\text{-}04$; Hippocampus, $r = -0.056$, $p = 0.0053$; AC, $r = -0.04$, $p = 0.0358$. To exclude potential confounds of load on RT (the larger the load, the longer the RT), we repeated a linear mixed effects model analysis after first classifying RTs as below/above the median RT for each load of a given patient – this analysis yielded nearly identical results to the original one.

A

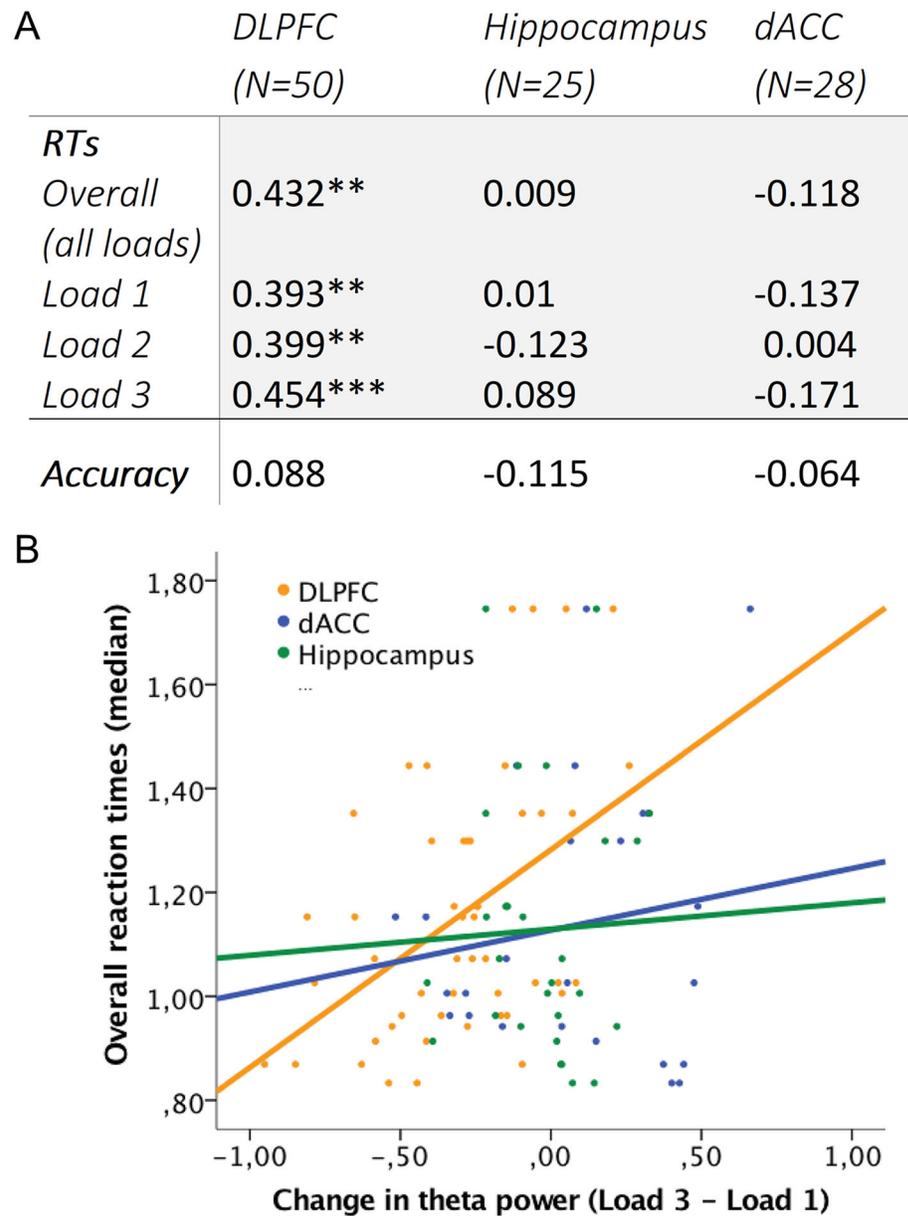|	DLPFC (N=50)	Hippocampus (N=25)	dACC (N=28)
RTs			
Overall (all loads)	0.432**	0.009	-0.118
Load 1	0.393**	0.01	-0.137
Load 2	0.399**	-0.123	0.004
Load 3	0.454***	0.089	-0.171
Accuracy	0.088	-0.115	-0.064

B

Figure 10. Change in theta power in DLPFC as a predictor of individual differences in WM performance.
(A) Correlation coefficients between the amount of theta power change and task performance (RT and accuracy). (B) Correlations between theta power change with memory load and individual patient's reaction times for each area. Each dot is an electrode.

Table 1.

Characteristics of participants included in this study.

ID	AGE	SEX	EPILEPSY DIAGNOSIS
P 34 [*]	70	M	bilateral mesial temporal
P 35 [*]	63	M	left temporal neocortical
P 36 [*]	45	M	right hippocampus
P 37 [*]	33	F	right hippocampus
P 39 [*]	26	M	right insula
P 40 [*]	25	M	right motor cortex
P 42	25	F	not localized
P 43	42	F	left hippocampus
P 44	53	F	right medial temporal
P 47	32	M	right mesial temporal
P 48	32	F	left amygdala
P 49	24	F	amygdala
P 51	17	M	not localized

[*]
The behavioral and single-neuron data from these patients are also part of (Kami ski et al., 2017), but the depth electrode recordings analyzed here are unpublished in all patients included.

Table 2.

Coordinates for each electrode used in analyses.

ID	RIGHT DLPFC	LEFT DLPFC	RIGHT HIPP	LEFT HIPP	RIGHT DACC	LEFT DACC
P 34	43.78, 23.23, 23.43; 49.08, 23.85, 23.43	−40.73, 24.47, 24.95; −47.43, 25.45, 25.10	30.56, −16.81, −16.47	−29.78, −17.97, −13.35	6.81, 21.20, 32.38	−7.20, 24.71, 29.13
P 35	40.72, 33.64, 30.99; 45.76, 34.48, 30.48	N/A	29.80, −14.88, −12.13	N/A	5.78, 29.40, 27.02	−6.83, 36.47, 27.02
P 36	43.24, 34.34, 21.69; 48.29, 34.24, 21.36	−39.89, 40.26, 24.02; −46.94, 40.07, 23.38	N/A	−31.43, −20.12, −14.96	9.15, 35.35, 22.12	−10.70, 36.91, 23.29
P 37	41.65, 21.43, 24.43; 46.89, 21.68, 25.31	−40.04, 27.72, 23.63; −45.28, 29.33, 23.63	28.83, −20.52, −13.51	−30.27, −19.20, −12.19	7.96, 20.70, 23.04	−10.78, 24.45, 23.37
P 39	43.26, 26.67, 22.42; 49.53, 28.48, 24.65	−37.24, 25.88, 15.70; −43.26, 25.88, 15.56	32.51, −26.99, −10.51	−28.92, −18.21, −12.85	14.70, 25.70, 24.68	−5.25, 27.04, 23.46
P 40	48.15, 24.17, 24.49; 52.79, 24.08, 25.23	−46.00, 27.42, 21.47; −50.23, 27.42, 21.82	33.93, −19.63, −10.91	−30.49, −20.39, −16.20	12.07, 28.21, 26.50	−8.53, 23.81, 20.78
P 42	45.07, 28.97, 24.49; 49.52, 28.97, 24.49	−41.64, 32.06, 22.09; −47.47, 32.40, 22.09	30.59, −21.51, −8.30	−24.64, −21.10, −12.78	6.81, 28.80, 24.92	−3.95, 28.42, 19.54
P 43	43.70, 24.70, 22.77; 49.86, 24.02, 23.12	−43.01, 27.10, 22.43; −48.49, 28.29, 23.12	31.40, −24.80, −14.60	−30.15, −20.34, −12.68	8.76, 26.85, 23.89	−5.25, 23.95, 23.39
P 44	43.40, 31.42, 16.99; 49.93, 29.92, 16.99	−43.10, 37.38, 15.36; −48.48, 36.63, 14.46	29.40, −21.70, −19.07	−25.29, −16.88, −17.11	5.20, 30.60, 18.63	−10.68, 36.48, 20.17
P 47	40.95, 30.18, 17.46; 46.49, 30.18, 17.77	N/A	30.37, −18.10, −18.10	−30.86, −17.82, −14.70	8.12, 26.02, 16.64	−3.89, 25.92, 20.00
P 48	44.31, 37.38, 18.41; 50.25, 37.07, 18.28	−38.58, 30.60, 25.32; −44.93, 30.12, 23.90	N/A	−34.46, −14.83, −15.94	11.72, 38.61, 17.97	−5.88, 28.68, 24.07
P 49	N/A	−40.01, 37.91, 21.56; −45.03, 37.91, 20.54	29.25, −17.87, −14.78	−24.15, −18.71, −19.93	9.56, 31.04, 26.12	−11.37, 33.91, 25.24
P 51	41.79, 31.65, 26.49; 46.88, 30.53, 25.62	−43.58, 32.35, 26.67; −48.68, 32.35, 26.26	29.86, −17.98, −13.83	−30.47, −19.73, −16.72	11.90, 31.65, 25.50	−8.78, 31.45, 28.02
AVG	X: 46.05 (3.4) Y: 28.97 (4.79) Z: 22.95 (3.84)	X: −44.09 (3.67) Y: 31.32 (5.02) Z: 21.93 (3.59)	X: 30.59 (1.52) Y: −20.07 (3.55) Z: −13.83 (3.28)	X: −29.24 (3.06) Y: −18.78 (1.77) Z: −14.95 (2.33)	X: 9.12 (2.8) Y: 28.8 (5.06) Z: 23.8 (4.25)	X: −7.62 (2.7) Y: 29.4 (5.06) Z: −23.65 (3.08)

Table 3.

Summary of Theta power changes during maintenance in Sternberg-like tasks in previously published human intracranial studies.

STUDY	LOCALIZATION OF THE EFFECT	METHOD	TASK	TASK EFFECT (VS BASELINE)	LOAD EFFECT
HOWARD ET AL., 2003	Temporal/frontal, occipital	iEEG	Verbal Sternberg	Mixed effects, some channels increase, some decrease – inconclusive (according to the authors)	Not explored in theta (visible in gamma)
RAGHAVACHARI ET AL., 2001	74 electrodes of 247 (24 in the temporal lobe, 18 in the occipital lobe, 18 in the parietal/motor/premotor areas, and 14 in the frontal lobe	iEEG	Verbal Sternberg	Mixed effects, mostly increase but on subject showed decrease at some trials	Not explored
RAGHAVACHARI ET AL., 2006	Occipital/parietal (45/157) ; temporal (23/280) frontal (2/182).	Subdural and depths	Verbal Sternberg	Increase of power	Not explored
Axmacher et al., 2010	Hippocampus	iEEG	Visual Sternberg	No data	No load related power effects
MELTZER ET AL., 2008	Midline and lateral part of PFC	iEEG	Numerical Sternberg	No data	Midline frontal sites: Increase in theta/alpha Lateral frontal sites: Decrease in theta/alpha
Van vugt et al., 2010	Prefrontal cortex and hippocampus	Subdural and depths	Sternberg with faces and letters	Not explored	Left lateral PFC – decrease for faces [40% of contacts], not letters [shown only in Fig. 2] Hippocampus – increase, right – 20% of contacts, left 15% [shown in Fig. 2 as well as in Table 2]